

Silver Nanoparticles Synthesized from *Phlogacanthus turgidus* Leaf Extract: Catalytic Activity in TMB-H₂O₂ Redox Reactions and their Application in Hydrogen Peroxide Sensing

Dang Van Su^{1,*}, Phan Thi Thanh Dieu¹, Nguyen Le Kim Thuy², Nguyen Thanh Danh²



Use your smartphone to scan this QR code and download this article

ABSTRACT

Introduction: Among metal nanoparticles (MNPs), silver nanoparticles (AgNPs) have attracted particular attention because of their excellent electrical and optical properties. Notably, colorimetric sensors incorporating metal nanoparticles have garnered significant attention from scientists in biochemical analysis, offering a simple solution. Here, we report the use of AgNPs in a hydrogen peroxide (H₂O₂) sensor. **Methods:** AgNPs were synthesized from *Phlogacanthus turgidus* leaf extract, H₂O₂ was used to oxidize colorless 3,3',5,5'-tetramethylbenzidine (TMB) into blue ox-TMB, and the reaction was catalyzed by AgNO₃. Measuring the resulting solution spectrophotometrically helped to determine the concentration of ox-TMB, thereby determining the concentration of H₂O₂ produced. **Results:** The UV-Vis spectrum of the AgNPs synthesized from *Phlogacanthus turgidus* leaf extract exhibited a prominent absorption peak at 427 nm. The linear range was determined to be 100–300 μM. The linear regression equation is $y = 0.91574 + 3.10484 \times 10^{-4} C_{H_2O_2}$, with an SD value of 0.00438. The results revealed that the limit of detection (LOD) of H₂O₂ through the color reaction between TMB and H₂O₂ in AgNP catalysis was 46.55 μM, and the limit of quantification (LOQ) was 141.07 μM. **Conclusion:** On the basis of the results of the optimal conditions for TMB oxidation in the presence of AgNPs, we can evaluate the applicability of this material as a H₂O₂ sensor.

Key words: AgNPs, green synthesis, *Phlogacanthus turgidus*, H₂O₂ sensor

¹Ho Chi Minh City University of Industry and Trade

²Institute of Chemical Technology, Vietnam Academy of Science and Technology

Correspondence

Dang Van Su, Ho Chi Minh City University of Industry and Trade

Email: sudv@huit.edu.vn

History

- Received: 2024-07-30
- Revised: 2024-12-11
- Accepted: 2024-12-27
- Published Online: 2024-12-31

DOI :



Copyright

© VNUHCM Press. This is an open-access article distributed under the terms of the Creative Commons Attribution 4.0 International license.



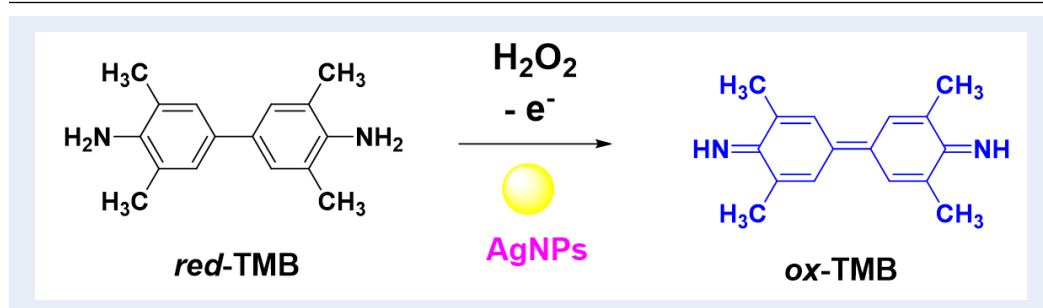
1 INTRODUCTION

MNPs have recently become a topic of interest because of their diverse applications^{1–6}. MNPs are important materials used in the fields of biomedicine, optics, the environment, catalysis and electrochemistry, such as biosensors^{7–11}. Among MNPs, AgNPs have received particular attention because of their excellent electrical and optical properties¹². H₂O₂ is a powerful oxidizing agent with various applications in medicine and industry. It is commonly known as a bleaching and disinfecting agent. However, proper handling is crucial to ensure safety and effectiveness, as it is highly corrosive and can alter stem cells and pose acute and chronic toxicity risks to aquatic environments^{13–15}. H₂O₂ is measured and quantified across a wide range of sample matrices, including environmental samples (water and soil), human fluids (sweat and blood), and cell and tissue cultures. Various methods are employed for this purpose, including optical techniques (colorimetry, chemiluminescence, and fluorescence), as well as electrochemical methods (potentiometry, voltammetry, and amperometry). Notably, colorimetric sensors incorporating

metal nanoparticles have garnered significant attention from scientists in biochemical analysis, offering a simple solution¹⁶.

Recently, many studies have investigated the green synthesis and application of AgNPs in H₂O₂ sensors. Nurul Ismillayli et al. (2024) reported the use of microwave-assisted synthesis of AgNPs as a colorimetric sensor for H₂O₂¹⁷. Ramesh Vinayagam et al. (2024) studied the structural characterization of marine macroalgae-derived AgNPs and their colorimetric sensing of H₂O₂¹⁸. Haodong Shen et al. (2023) reported a one-step synthesis of nanosilver embedding laser-induced graphene for H₂O₂ sensors¹⁹. However, there has been no research on the synthesis of AgNPs from *Phlogacanthus turgidus* leaf extract for application as H₂O₂ detectors on the basis of the reduction reactions of TMB and H₂O₂ in AgNP catalysis. The reduction in TMB is illustrated in Scheme 1. In this strategy, the AgNPs act as catalysts, and the oxidation product of TMB possesses a blue color, which can be determined via UV-Vis spectroscopy. The catalytic mechanism of AgNPs involves three primary steps: (1) the generation of hydroxyl radicals (OH[•]),

Cite this article : Su DV, Dieu PTT, Thuy NLK, Danh NT. Silver Nanoparticles Synthesized from *Phlogacanthus turgidus* Leaf Extract: Catalytic Activity in TMB-H₂O₂ Redox Reactions and their Application in Hydrogen Peroxide Sensing. *Sci. Tech. Dev. J.* 2025; 27(4):1-9.



Scheme 1: Oxidation mechanism of TMB using H₂O₂ in the presence of a AgNP catalyst.

47 (2) the production of oxygen (O₂), and (3) electron
 48 transfer, as illustrated in Scheme 1²⁰. Moreover, the
 49 extract of the *Phlogacanthus turgidus* leaf contains
 50 high levels of polyphenols²¹, which have the ability
 51 to reduce and stabilize metallic nanoparticles. In this
 52 study, *Phlogacanthus turgidus* leaf extract was used to
 53 synthesize AgNPs, and the catalytic ability of AgNPs
 54 in the redox reaction between H₂O₂ and TMB was in-
 55 vestigated.

56 MATERIALS AND METHODS

57 Materials

58 *Phlogacanthus turgidus* leaves were collected from Bu
 59 Gia Map National Park, Binh Phuoc Province, Viet-
 60 nam. Chemicals including silver nitrate (AgNO₃),
 61 3,3',5,5'-tetramethylbenzidine (C₁₆H₂₀N₂), hydrogen
 62 peroxide (H₂O₂), acetic acid (CH₃COOH) and
 63 sodium acetate (CH₃COONa), which were of ana-
 64 lytical grade without further purification, were pur-
 65 chased from Acros Co., Belgium. Deionized water
 66 was thoroughly utilized in all the experiments.

67 Methods

68 Synthesis of AgNPs from *Phlogacanthus* 69 *turgidus* leaf extract

70 The synthesis of silver nanoparticles (AgNPs) was
 71 performed via *Phlogacanthus turgidus* leaf extract, fol-
 72 lowing previous reports^{2,5}. Specifically, 0.25 mL of
 73 *Phlogacanthus turgidus* leaf extract was mixed with
 74 5 mL of an aqueous AgNO₃ solution under reaction
 75 conditions of 2.0 mM silver ion concentration, 80°C,
 76 and a reaction time of 70 minutes. The formation
 77 of AgNPs was verified via UV-Vis spectrophotome-
 78 try. The synthesized AgNP solution was subsequently
 79 stored at 8°C for future applications.

80 Determination of the optimal temperature 81 for the TMB and H₂O₂ reactions with the 82 AgNP catalyst

83 To optimize the reaction temperature, 400 μL of 5
 84 mM TMB, 2 mL of acetate buffer solution (pH 5),
 85 600 μL of 400 μM H₂O₂, and 150 μL of the synthe-
 86 sized AgNP solution were each carefully added to a
 87 10 mL bottle. The bottle was covered with foil to pro-
 88 tect it from light and placed in a thermostatic bath at
 89 various temperatures (30°C, 35°C, 40°C, 45°C, 50°C,
 90 55°C, and 60°C) for 30 minutes. Following incubation,
 91 UV-Vis spectroscopy was used to measure the
 92 absorbance of the solutions to determine the optimal
 93 temperature for the reaction of TMB and H₂O₂ in the
 94 presence of the AgNP catalyst.

95 Determination of the optimal time for the 96 TMB and H₂O₂ reactions with the AgNP cat- 97 alyst

98 To determine the optimal reaction time, 400 μL of 5
 99 mM TMB, 2 mL of acetate buffer solution (pH 5), 600
 100 μL of 400 μM H₂O₂, and 150 μL of the AgNP solu-
 101 tion were added to a 10 mL container, which was care-
 102 fully covered with foil. This container was then placed
 103 in a thermostatic reaction tank set to the optimal tem-
 104 perature. UV-Vis spectroscopy measurements were
 105 taken at 10-minute intervals to identify the optimal
 106 reaction time for the interaction between TMB and
 107 H₂O₂ in the presence of the AgNP catalyst.

108 Determination of the optimal pH for the TMB 109 and H₂O₂ reactions with the AgNP catalyst

110 To optimize the pH for the reaction, 400 μL of 5 mM
 111 TMB, 2 mL of acetate buffer solution at various pH
 112 values, 600 μL of 400 μM H₂O₂, and 150 μL of the
 113 AgNP solution were added to 10 mL bottles and cov-
 114 ered with foil. These bottles were then placed in a
 115 thermostatic bath set to the optimal temperature and

time. UV-Vis spectroscopy measurements were conducted to identify the optimal pH for the TMB and H₂O₂ reactions in the presence of the AgNP catalyst.

Determination of the optimal AgNP concentration for the TMB and H₂O₂ reactions with the AgNP catalyst

To optimize the concentration of AgNPs, 400 μL of 5 mM TMB, 2 mL of acetate buffer solution (adjusted to the optimal pH), 600 μL of 400 μM H₂O₂, and varying volumes of the AgNP solution (60 μL, 70 μL, 80 μL, 90 μL, 100 μL, 110 μL, 120 μL, and 130 μL) were added to separate 10 mL bottles, each covered with foil. These bottles were then placed in a thermostatic bath set to the optimal temperature and time. UV-Vis spectroscopy was used to determine the optimal concentration of AgNPs for the TMB and H₂O₂ reactions.

Determination of the optimal TMB concentration for TMB and H₂O₂ reactions with AgNP catalysts

To determine the optimal concentration of TMB, 2 mL of acetate buffer solution (adjusted to the optimal pH), 600 μL of 400 μM H₂O₂, the optimal volume of AgNP solution (determined in section 2.5), and varying concentrations of TMB (400 μL of 3 mM, 3.5 mM, 4 mM, 4.5 mM, 5 mM, 5.5 mM, 6 mM, or 6.5 mM) were added to separate 10 mL bottles, which were covered with foil. These bottles were then placed in a thermostatic bath set to the optimal temperature and time. UV-Vis spectroscopy was performed to determine the optimal TMB concentration for the TMB and H₂O₂ reactions catalyzed by the AgNPs.

Determination of the linear range and limit of detection (LOD) value

To determine the optimal concentration of H₂O₂, 400 μL of TMB, 2 mL of acetate buffer solution (adjusted to the optimal pH), and the optimal volume of AgNP solution were combined with varying concentrations of H₂O₂ (600 μL of 10 μM, 50 μM, 100 μM, 150 μM, 200 μM, 250 μM, 300 μM, 350 μM, and 400 μM) in separate 10 mL bottles, each covered with foil. These bottles were placed in a thermostatic bath set to the optimal temperature and time. UV-Vis spectroscopy was conducted on the solutions to identify the optimal concentration of H₂O₂ for the reaction with TMB catalyzed by AgNPs. The limits of detection (LODs) and limits of values were calculated via Equations (1) and

(2), respectively:

$$LOD = 3.3 \times \frac{SD}{a} = 3.3 \times \frac{0.0438}{3.10484 \times 10^{-4}} = 46.55 \mu M \quad (1)$$

$$LOQ = 10 \times \frac{SD}{a} = 10 \times \frac{0.0438}{3.10484 \times 10^{-4}} = 141.07 \mu M \quad (2)$$

where SD and a are the standard deviation and slope of the linear regression line, respectively.

RESULTS AND DISCUSSION

Synthesis of AgNPs from *Phlogacanthus turgidus* leaf extract

Figure 1a shows that the peak absorption of the AgNPs synthesized from *Phlogacanthus turgidus* leaf extract was in the wavelength range of 400–500 nm. The UV-Vis spectrum of the AgNPs synthesized from *Phlogacanthus turgidus* leaf extract exhibited a surface plasmon resonance (SPR) peak at 427 nm. Microscopy images (Figure 1b and Figure 1c) revealed that the structure of the AgNPs consisted mostly of spheres with an average size of 13 nm, which aligns with the findings of a previous study².

Optimization of the TMB and H₂O₂ reactions with the AgNP catalyst

Figure 2 shows the UV-Vis spectra of TMB oxidation as a function of reaction temperature. The absorption spectra were recorded over a temperature range from 20°C to 60°C. The data indicated that the absorbance at a wavelength of 654 nm increased progressively with temperature, reaching a maximum at 35°C. Beyond this temperature, a decrease in absorbance was observed, which was likely attributed to the thermal instability of ox-TMB at higher temperatures. Accordingly, 35°C was identified as the most favorable temperature for the efficient oxidation of TMB by H₂O₂, facilitated by the AgNP catalyst.

Results of the optimal time for the reaction of TMB and H₂O₂ with the AgNP catalyst

The effect of reaction time on TMB oxidation was evaluated at the optimal temperature of 35°C, with measurements taken at 10-minute intervals to identify the optimal reaction duration. The absorbance data obtained via UV-Vis spectroscopy are presented in Figure 3. Superimposing the absorption spectra for various time points revealed that the reaction

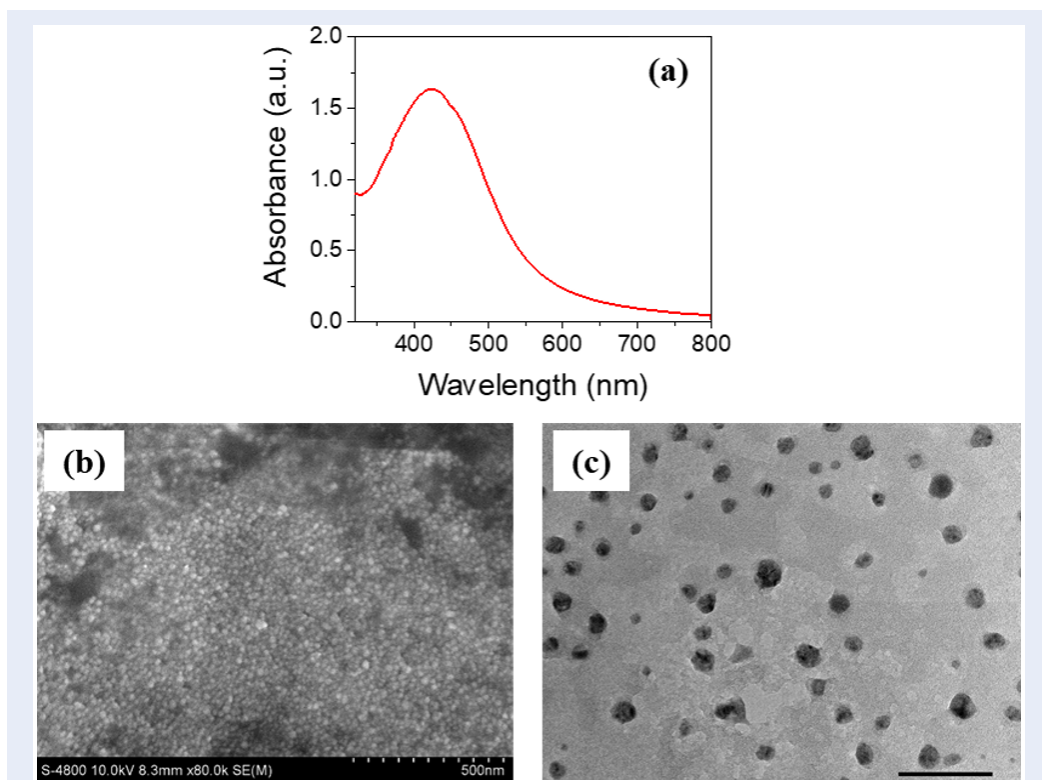


Figure 1: UV-Vis spectra (a) and SEM (b) and TEM (c) images of AgNPs synthesized from *Phlogacanthus turgidus* leaf extract

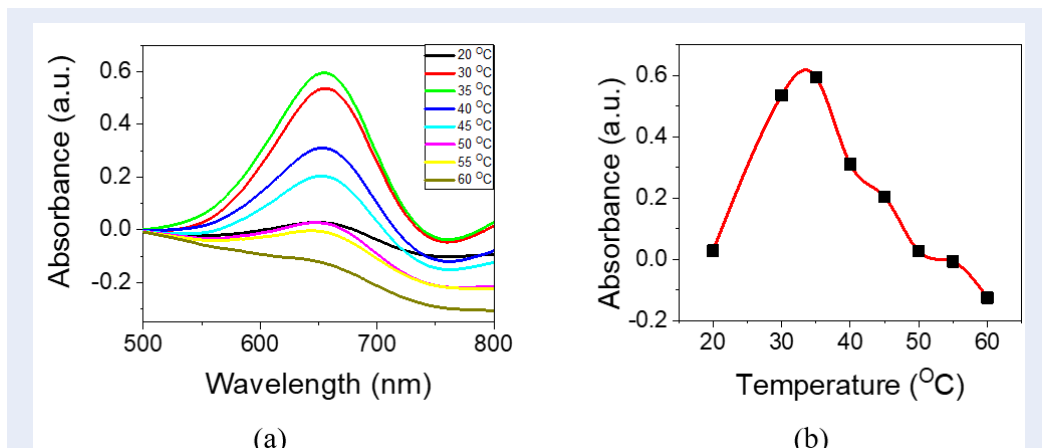
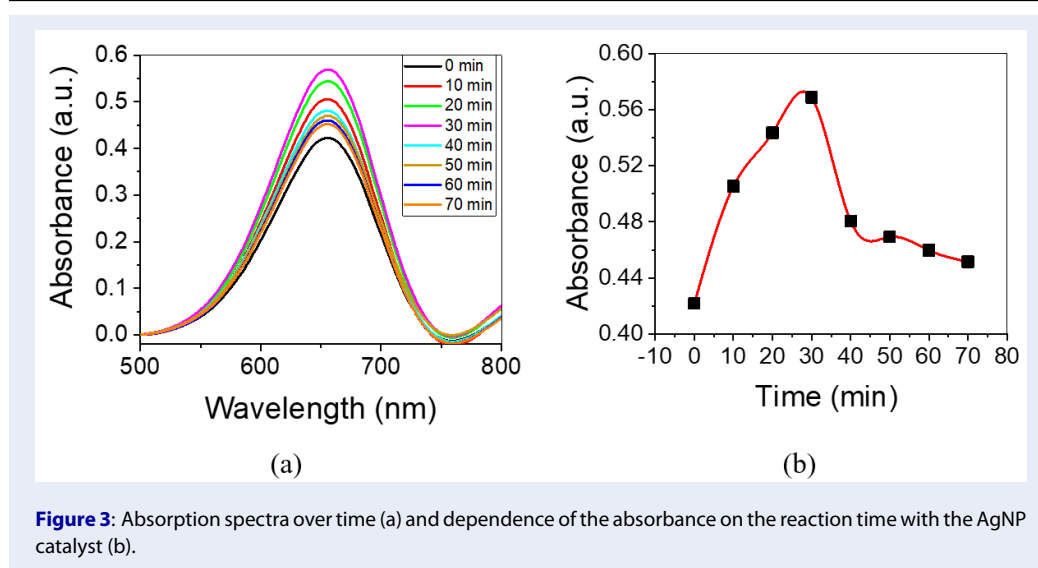


Figure 2: Absorption spectra from the temperature investigation with the AgNP catalyst (a) and the dependence of the absorbance on the reaction temperature (with the AgNP catalyst) (b).



202 conducted for 30 minutes presented the highest absor-
 203 bance intensity at 654 nm. This observation sugges-
 204 ts that extended reaction times under these condi-
 205 tions may lead to the degradation of *ox*-TMB. There-
 206 fore, a reaction time of 30 min was determined to be
 207 the most suitable condition for the oxidation of TMB
 208 by H₂O₂ in the presence of the AgNP catalyst, start-
 209 ing from the moment the sample was introduced into
 210 the thermostatic bath.

211 **Results of the optimal pH for the reaction of**
 212 **TMB and H₂O₂ with the AgNP catalyst**

213 pH plays a principal role in regulating the oxidation
 214 rate of TMB. UV-Vis spectra were recorded and com-
 215 pared for samples prepared under various pH condi-
 216 tions, as illustrated in Figure 4. The data revealed
 217 that samples with a pH of 4 presented the highest
 218 absorbance intensity at 654 nm, while this intensity
 219 progressively decreased for samples with low or high
 220 pH values. This trend can be attributed to the reac-
 221 tion equilibrium under highly acidic conditions (pH <
 222 4.0) shifting toward the formation of *red*-TMB. Con-
 223 versely, at higher pH values, the decreasing forma-
 224 tion efficiency of the colored product at 654 nm may
 225 result from the elevated redox potential of the sub-
 226 strates, leading to decreased susceptibility to oxida-
 227 tion²². Consequently, pH 4 was identified as the op-
 228 timal condition and was selected for further explo-
 229 ration of the factors influencing the TMB redox pro-
 230 cess with H₂O₂ in the presence of an AgNP catalyst.

231 **The effects of the optimal AgNP concentra-**
 232 **tion on the TMB and H₂O₂ reactions**

233 A survey was conducted to investigate the influence
 234 of the AgNP catalyst volume on the absorption inten-
 235 sity of the samples in solution. The absorption spec-
 236 tra of the solutions containing TMB, acetate buffer
 237 (pH 4), H₂O₂, and various volumes of the AgNP cat-
 238 alyst were analyzed (Figure 5). At a wavelength of
 239 654 nm, the absorption intensity increased progres-
 240 sively as the AgNP volume increased from 60 μL to
 241 120 μL under constant conditions of TMB concentra-
 242 tion, acetate buffer, and H₂O₂. However, a significant
 243 decrease in the absorption intensity was observed in
 244 the sample containing 130 μL of the AgNP catalyst.
 245 This indicated that increasing the catalyst volume in-
 246 creased the surface area, thereby improving the cataly-
 247 tic efficiency of the oxidation-reduction reaction.
 248 Nevertheless, an excessive amount of AgNPs likely re-
 249 sulted in the decomposition of H₂O₂, reducing the re-
 250 action yield. Therefore, 120 μL of AgNP catalyst was
 251 identified as the optimal volume and was selected for
 252 subsequent investigations of other reaction param-
 253 eters.

254 **The effects of the optimal TMB concentra-**
 255 **tion on the TMB and H₂O₂ reactions with**
 256 **the AgNP catalyst**

257 The TMB concentration is a critical parameter for
 258 evaluating the reaction efficiency between TMB and
 259 H₂O₂ in the presence of the synthesized AgNP cat-
 260 alyst. Figure 6 shows the dependence of the reac-
 261 tion efficiency on the TMB concentration through
 262 changes in the absorption intensity observed in the

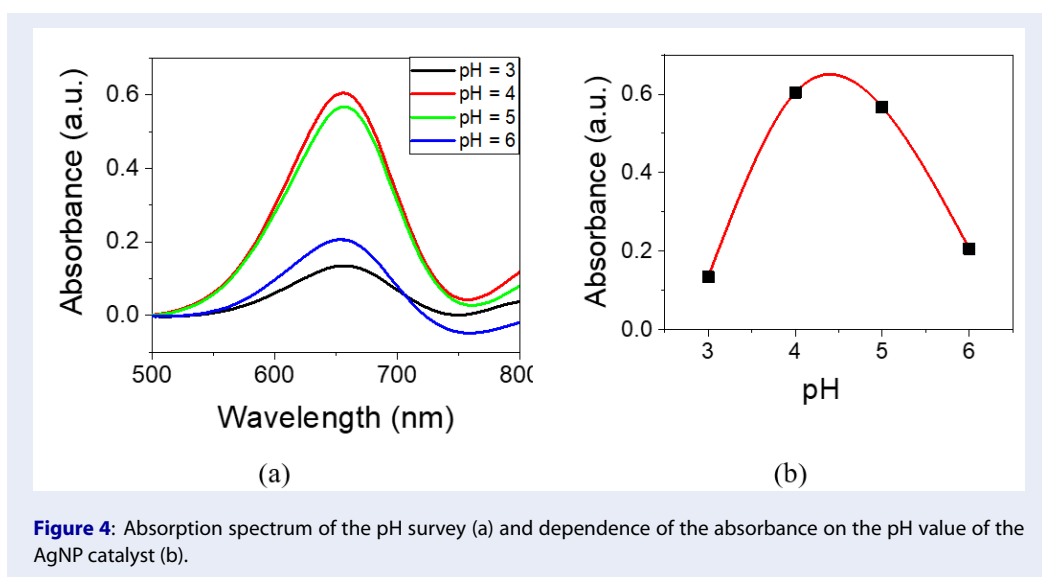


Figure 4: Absorption spectrum of the pH survey (a) and dependence of the absorbance on the pH value of the AgNP catalyst (b).

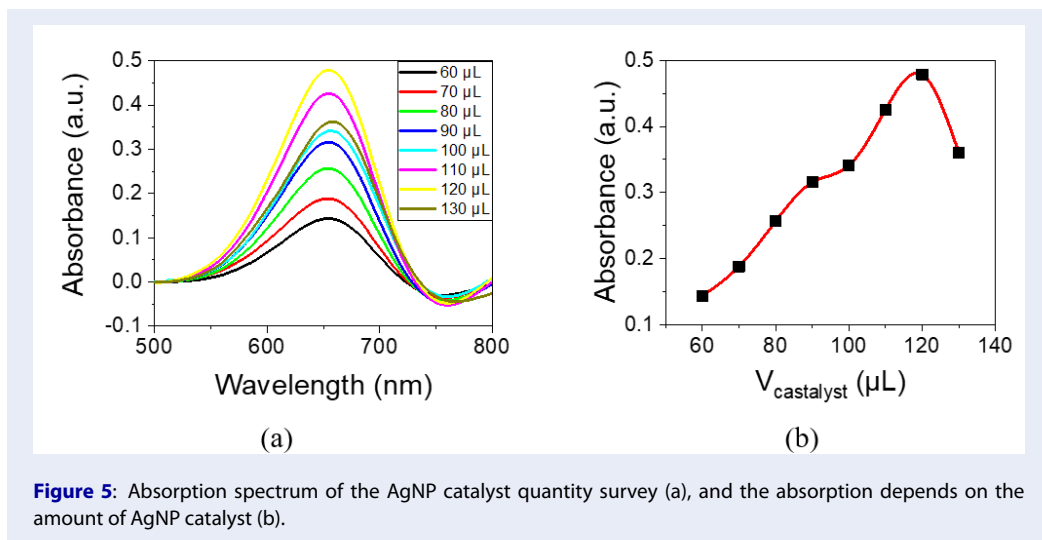


Figure 5: Absorption spectrum of the AgNP catalyst quantity survey (a), and the absorbance depends on the amount of AgNP catalyst (b).

263 UV-Vis spectra at 654 nm. The results revealed
 264 that the absorbance intensity increased with increas-
 265 ing TMB concentration, reaching a maximum at 5.5
 266 mM. Above this concentration, the absorbance de-
 267 creased significantly, likely due to the oxidation of
 268 monoamine groups in TMB at higher concentrations.
 269 Consequently, a TMB concentration of 5.5 mM was
 270 selected as the optimal condition for the redox reac-
 271 tion between TMB and H₂O₂ in the presence of the
 272 AgNP catalyst.

Influence of the H₂O₂ concentration on the TMB and H₂O₂ reactions with the AgNP catalyst

273 Figure 7 shows the dependence of the absorbance val-
 274 ues on the H₂O₂ concentration. The absorbance in-
 275 tensity at 654 nm increased with increasing H₂O₂
 276 concentration, reaching a maximum at 350 µM. Be-
 277 yond this concentration, the TMB concentration ap-
 278 peared insufficient to react fully with H₂O₂. A linear
 279 relationship was observed within the range of 100-
 280 300 µM, described by the regression equation $y = 0.91574 + 3.10484 \times 10^{-4} C_{H_2O_2}$, with a standard
 281 deviation (SD) of 0.00438. The limit of detection (LOD)
 282 for H₂O₂, which is based on the colorimetric reac-
 283 tion between oxidized TMB (ox-TMB) and H₂O₂
 284
 285
 286
 287

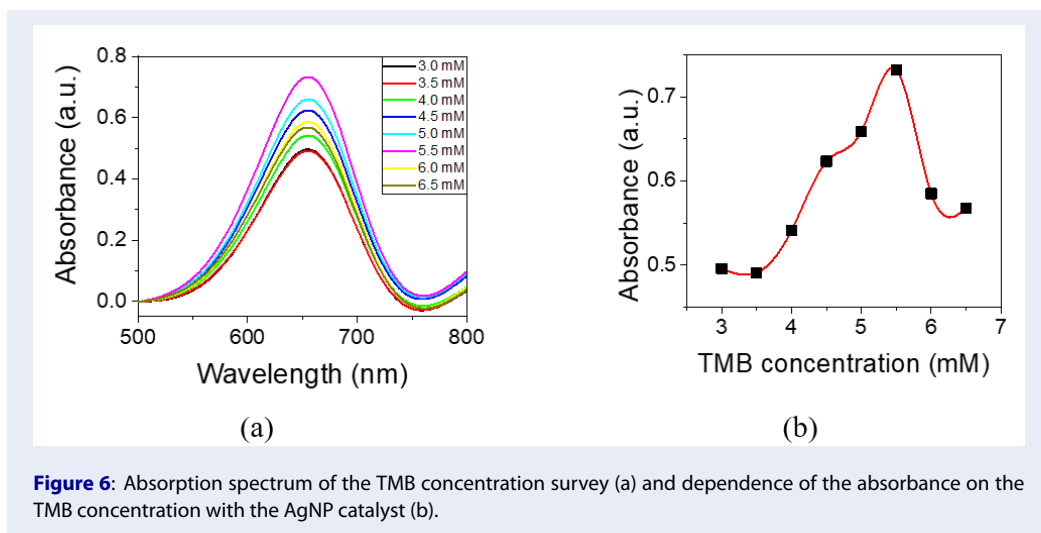


Figure 6: Absorption spectrum of the TMB concentration survey (a) and dependence of the absorbance on the TMB concentration with the AgNP catalyst (b).

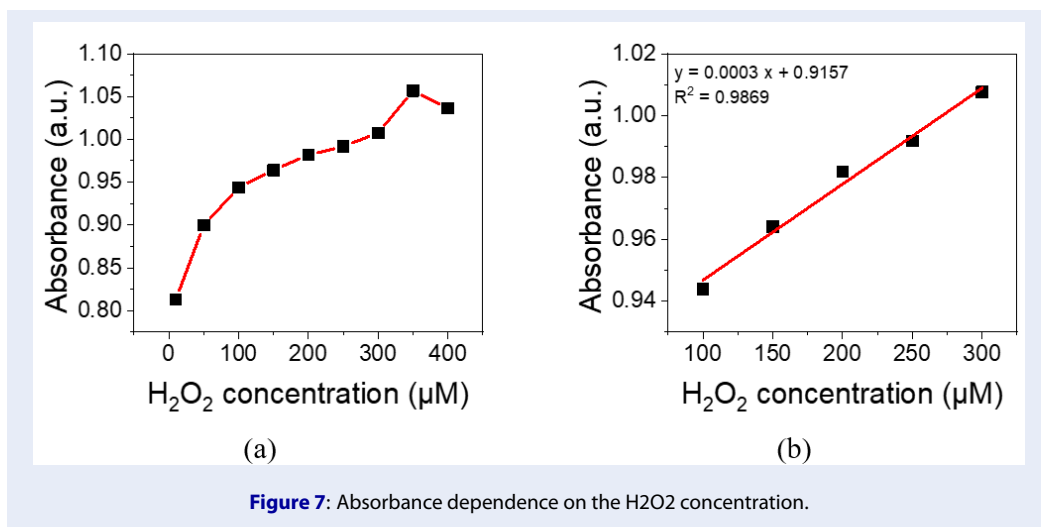


Figure 7: Absorbance dependence on the H₂O₂ concentration.

288 catalyzed by AgNPs, was determined to be 46.55 μM, 304
 289 with a limit of quantification (LOQ) of 141.07 μM. 305
 290 These findings, combined with the optimal conditions 306
 291 for TMB oxidation shown in Table 1, underscore the 307
 292 potential of AgNPs as effective catalysts in the TMB- 308
 293 H₂O₂ redox reaction, demonstrating their applicabil- 309
 294 ity as sensitive H₂O₂ sensors.

295 **CONCLUSIONS**

296 AgNPs were synthesized from *Phlogacanthus turgidus* 310
 297 leaf extract, resulting in absorption peaks in the wave- 311
 298 length range of 400–500 nm. This investigation of the 312
 299 conditions affecting the oxidation of TMB with H₂O₂ 313
 300 with the AgNP catalyst provides the best conditions 314
 301 for the detection of H₂O₂ through the TMB reaction 315
 302 with the AgNP catalyst. The optimal conditions (tem-
 303 perature, time, pH, AgNP concentration, TMB con-

centration, and H₂O₂ concentration) for TMB oxida-
 tion in the presence of H₂O₂ were 35°C, 30 min, pH
 4, 120 μL of AgNPs, 5.5 mM TMB, and H₂O₂ con-
 centrations ranging from 100–300 μM. Therefore, we
 can evaluate the applicability of H₂O₂ in wastewater.

310 **ABBREVIATIONS**

311 xxx

312 **ACKNOWLEDGMENTS**

313 xxx

314 **AUTHOR'S CONTRIBUTIONS**

315 xxx

Table 1: Optimal conditions for TMB oxidation in the presence of AgNPs.

Parameters	Optimal values
Temperature (°C)	35
Time (minute)	30
pH	4.0
AgNPs catalyst (μL)	120
TMB (mM)	5.5
Concentration range linear H2O2 (μM)	100 - 300

FUNDING

This research is funded by the Vietnam National Foundation for Science and Technology Development (NAFOSTED) under grant number 104.99–2021.56

AVAILABILITY OF DATA AND MATERIALS

Data and materials used and/or analyzed during the current study are available from the corresponding author on reasonable request.

ETHICS APPROVAL AND CONSENT TO PARTICIPATE

Not applicable.

CONSENT FOR PUBLICATION

Not applicable.

COMPETING INTERESTS

The authors declare that they have no competing interests.

REFERENCES

1. Ân TNM. Tổng hợp xanh Nano bạc từ AgNO₃ và dịch chiết lá diếp cá. *Tp.* 2016;32:188–92;.

2. Dang VS, Tran HH, Dieu PTT, Tran MT, Dang CH, Mai DT, et al. Effective catalysis and antibacterial activity of silver and gold nanoparticles biosynthesized by *Phlogacanthus turgidus*. *Res Chem Intermed* [Internet]. 2022;48(5):2047–67; Available from: <https://doi.org/10.1007/s11164-022-04687-9>.

3. Ruddaraju LK, Pallela PNVK, Pammi SVN, Padavala VS, Kolapalli VRM. Synergetic antibacterial and anticarcinogenic effects of *Annona squamosa* leaf extract mediated silver nano particles. *Mater Sci Semicond Process* [Internet]. 2019;100(April):301–9; Available from: <https://doi.org/10.1016/j.mssp.2019.05.007>.

4. Saad PG, Castélin RD, Ravi V, Al-Amri IS, Khan SA. Green synthesis of silver nanoparticles using Omani pomegranate peel extract and two polyphenolic natural products: characterization and comparison of their antioxidant, antibacterial, and cytotoxic activities. *Beni-Suef Univ J Basic Appl Sci.* 2021;10(1);.

5. Nguyen TTN, Vo TT, Nguyen BNH, Nguyen DT, Dang VS, Dang CH, et al. Silver and gold nanoparticles biosynthesized by aqueous extract of burdock root, *Arctium lappa* as antimicrobial agent and catalyst for degradation of pollutants. *Environ*

Sci Pollut Res. 2018;25(34):34247–61;.

6. Vo TT, Nguyen TTN, Huynh TTT, Vo TTT, Nguyen TTN, Nguyen DT, et al. Biosynthesis of silver and gold nanoparticles using aqueous extract from *crinum latifolium* leaf and their applications forward antibacterial effect and wastewater treatment. *J Nanomater.* 2019;2019:1–14;.

7. Bandi R, Alle M, Park CW, Han SY, Kwon GJ, Kim JC, et al. Rapid synchronous synthesis of Ag nanoparticles and Ag nanoparticles/holocellulose nanofibrils: Hg(II) detection and dye discoloration. *Carbohydr Polym* [Internet]. 2020;240(March):116356; Available from: <https://doi.org/10.1016/j.carbpol.2020.116356>.

8. Shipway AN, Katz E, Willner I. Nanoparticle arrays on surfaces for electronic, optical, and sensor applications. *Angew Chemie (International Ed English).* 2000;39(15 SUPPL.):19–52;.

9. Tracey CT, Torlopov MA, Martakov IS, Vdovichenko EA, Zhukov M, Krivoschapkin P V., et al. Hybrid cellulose nanocrystal/magnetite glucose biosensors. *Carbohydr Polym* [Internet]. 2020;247(February):116704; Available from: <https://doi.org/10.1016/j.carbpol.2020.116704>.

10. Mohammed FS, Cole SR, Kitchens CL. Synthesis and enhanced colloidal stability of cationic gold nanoparticles using polyethyleneimine and carbon dioxide. *ACS Sustain Chem Eng.* 2013;1(7):826–32;.

11. Wang F, Ding X, Niu X, Liu X, Wang W, Zhang J. Green preparation of core-shell Cu@Pd nanoparticles with chitosan for glucose detection. *Carbohydr Polym* [Internet]. 2020;247(February):116647; Available from: <https://doi.org/10.1016/j.carbpol.2020.116647>.

12. Bonigala B, Kasukurthi B, Konduri VV, Mangamuri UK, Gorepati R, Poda S. Green synthesis of silver and gold nanoparticles using *Stemona tuberosa* Lour and screening for their catalytic activity in the degradation of toxic chemicals. *Environ Sci Pollut Res.* 2018;25(32):32540–8;.

13. Phụ lục 17 - Kèm thông tư số 28/2010/TT-BCT ngày 28 tháng 6 năm 2010 của Bộ Công Thương. Bộ Công Thương. 2014;17:1–7;.

14. Eldridge D, Holstege CP. Hydrogen peroxide. *Chemwatch.* 2016;(7.1.1.1):1–13;.

15. Chen S, Yuan R, Chai Y, Hu F. Electrochemical sensing of hydrogen peroxide using metal nanoparticles: A review. *Microchim Acta.* 2013;180(1–2):15–32;.

16. Đồng Huy Giới, Bùi Thị Thu Hương, Phí Thị Cẩm Miện Nguyễn Thị Thủy Hạnh ĐĐN. Tạo cảm biến từ Nano vàng và ADN chức năng để phát hiện nhanh ion thủy ngân trong nước. *Tạp chí Khoa học nông nghiệp Việt Nam.* 2016;14(3):491–500;.

17. Ismailayli N, Suprpto S, Santoso E, Nugraha RE, Holilah H, Bahruji H, et al. Microwave-assisted synthesis of silver nanoparticles as a colorimetric sensor for hydrogen peroxide. *RSC Adv.* 2024;14(10):6815–22;.

18. Vinayagam R, Nagendran V, Goveas LC, Narasimhan MK, Varadavenkatesan T, Chandrasekar N, et al. Structural characterization of marine macroalgae derived silver nanoparticles and their colorimetric sensing of hydrogen peroxide. *Mater Chem Phys* [Internet]. 2024;313(December 2023):128787; Available

- 412 from: <https://doi.org/10.1016/j.matchemphys.2023.128787>.
- 413 19. Shen H, Liu J, Pan P, Yang X, Yang Z, Li P, et al. One-step
414 synthesis of nanosilver embedding laser-induced graphene
415 for H₂O₂ sensor. *Synth Met* [Internet]. 2023;293(Decem-
416 ber 2022):117235;Available from: [https://doi.org/10.1016/j.](https://doi.org/10.1016/j.synthmet.2022.117235)
417 [synthmet.2022.117235](https://doi.org/10.1016/j.synthmet.2022.117235).
- 418 20. An C zheng; WKTY and X. Intrinsic peroxidase-like activity and
419 the catalytic mechanism of gold @ carbon dots nanocompos-
420 ites. *RSC Adv*. 2013;00(1–3):1–8;.
- 421 21. Minh PN, Phát NT, Chí MT, Hiến ĐC, Trí MĐ. Thành phần
422 hóa học của toàn cây Thường sơn tía PHLOGACANTHUS
423 TURGIDUS (FUA EX HOOK . F.) LINDAU. 2021;5(3):1341–9;.
- 424 22. He W, Liu Y, Yuan J, Yin JJ, Wu X, Hu X, et al. Au@Pt nanos-
425 tructures as oxidase and peroxidase mimetics for use in
426 immunoassays. *Biomaterials* [Internet]. 2011;32(4):1139–
427 47;Available from: [http://dx.doi.org/10.1016/j.biomaterials.](http://dx.doi.org/10.1016/j.biomaterials.2010.09.040)
428 [2010.09.040](http://dx.doi.org/10.1016/j.biomaterials.2010.09.040).